Global Change Biology (2007) **13,** 108–122, doi: 10.1111/j.1365-2486.2006.01289.x

Changes in European ecosystem productivity and carbon balance driven by regional climate model output

PABLO MORALES*, THOMAS HICKLER*, DAVID P. ROWELL†, BENJAMIN SMITH* and MARTIN T. SYKES*

**Centre for Geobiosphere Science, Department of Physical Geography and Ecosystems Analysis, Lund University, Sölvegatan 12, S-223 62 Lund, Sweden, †Met Office, Hadley Centre for Climate Prediction and Research, Exeter EX1 3PB, UK*

Abstract

Climate change resulting from the enhanced greenhouse effect together with the direct effect of increased atmospheric CO_2 concentrations on vegetation growth are expected to produce changes in the cycling of carbon in terrestrial ecosystems. Impacts will vary across Europe, and regional-scale studies are needed to resolve this variability. In this study, we used the LPJ-GUESS ecosystem model driven by a suite of regional climate model (RCM) scenarios from the European Union (EU) project PRUDENCE to estimate climate impacts on carbon cycling across Europe. We identified similarities and discrepancies in simulated climate impacts across scenarios, particularly analyzing the uncertainties arising from the range of climate models and emissions scenarios considered. Our results suggest that net primary production (NPP) and heterotrophic respiration (Rh) will generally increase throughout Europe, but with considerable variation between European subregions. The smallest NPP increases, and in some cases decreases, occurred in the Mediterranean, where many ecosystems switched from sinks to sources of carbon by 2100, mainly as a result of deteriorating water balance. Over the period 1991–2100, modeled climate change impacts on the European carbon balance ranged from a sink of 11.6 Gt C to a source of 3.3 Gt C, the average annual sink corresponding with 1.85% of the current EU anthropogenic emissions. Projected changes in carbon balance were more dependent on the choice of the general circulation model (GCM) providing boundary conditions to the RCM than the choice of RCM or the level of anthropogenic greenhouse gases emissions.

Keywords: carbon flux, climate change, ecosystem model, LPJ-GUESS, NEE, NPP, regional climate model (RCM)

Received 5 January 2006; revised version received 26 June 2006 and accepted 12 July 2006

Introduction

The cycling of carbon between terrestrial ecosystems and the atmosphere is an essential biospheric process with feedbacks to the physical system at various spatial and temporal scales (Houghton *et al*., 1998; Waring & Running, 1998). Changes in vegetation patterns and net primary production (NPP), with associated changes in carbon fluxes and storage, are expected as a consequence of climatic changes driven by rising atmospheric concentrations of greenhouse gases (GHG; Cao & Woodward, 1998). Understanding the likely changes in European carbon exchange and storage is important for policy makers because carbon sinks in soil organic matter (SOM) and forests can be accounted for in the Kyoto Protocol (Conference of the Parties, 1998).

Process-based models have been widely used to study the role of the terrestrial biosphere in the global carbon cycle and to assess changes in biogeochemical cycles associated with a changing climate (e.g. Cramer *et al*., 2001; Bachelet *et al*., 2003; Fowler *et al*., 2003; Masera *et al*., 2003). Assessments of potential impacts of climate change on ecosystems in Europe using these models have generally relied on scenarios of future climate from general circulation model (GCM; Parry, 2000; Schröter *et al*., 2005; Schaphoff *et al*., 2006). Such

Correspondence: Present address: Pablo Morales, Department of Agricultural Economics, Faculty of Agricultural Sciences, Universidad de Chile, Santa Rosa 11.315, La Pintana, Santiago, Chile. Fax + 56 2 9785790, e-mail: pamorale@uchile.cl

GCM outputs have a coarse resolution (ca. 300 km), considerably coarser than the typical scale of variation in the impacts (Mearns *et al*., 2003). Process-based models of ecosystem responses are highly sensitive to fine-scale climate variations, especially in regions of complex topography and surface cover (e.g. the Alps, the Mediterranean or Scandinavia), and in areas with strong maritime influence (e.g. around the Baltic sea; IPCC, 2001). Therefore, if there is a need to assess the impacts of climate change on terrestrial ecosystems at a regional scale, then the coarse resolution of GCM is a serious limitation (O'Brien *et al*., 2004).

Climate scenarios with higher spatial resolution can be obtained using a nested regional climate model (RCM) driven by initial and boundary conditions supplied by a GCM (Mearns *et al*., 2003). An increasing number of RCM experiments have been used in a wide range of impact studies at different spatial scales in diverse regions of the world (e.g. Tsvetsinskaya *et al*., 2003; Arnell, 2004; Jha *et al*., 2004). However, although RCMs are more applicable for regional impact studies than GCMs, they suffer from uncertainties similar to those affecting GCM output. Crucially, RCMs are dependent on inputs from the driving GCM (Mearns *et al*., 2003). The uncertainties in projected impacts using RCMs are further affected by uncertainties in future GHG emissions scenarios used to drive them (Nakicenovic *et al*., 2000) and in the response of the different driving GCMs to a given external forcing such as increased atmospheric GHG concentrations (Räisänen *et al*., 2004; Déqué *et al*., 2006; Rowell, 2006). The effects of these uncertainties on ecosystem structure and functioning have been addressed based on GCM outputs (Cramer *et al*., 2001; Zheng *et al*., 2002). However, there is also a need to address these uncertainties at local and regional scales.

In this study, we used the LPJ-GUESS process-based ecosystem model (Smith *et al*., 2001; Sitch *et al*., 2003) and a suite of high-resolution RCM-based scenarios and their IPCC-SRES emission scenarios A2 and B2 from the European Union (EU) project PRUDENCE (Christensen *et al*., 2006) to assess the potential impacts of climate change and associated changes in atmospheric CO_2 concentrations on vegetation structure, NPP, net ecosystem carbon exchange (NEE) and terrestrial ecosystem carbon stocks in Europe. We analyze the uncertainties in the projected impacts, investigate similarities and discrepancies among scenarios and identify robust, qualitative regional patterns in carbon exchange and storage.

Materials and methods

The LPJ-GUESS ecosystem model

LPJ-GUESS (Smith *et al*., 2001; Sitch *et al*., 2003) is a model of the dynamics of ecosystem structure and functioning at scales from the patch to the globe. It incorporates process-based representations of plant physiology and ecosystem biogeochemistry, derived from the BIOME3 model (Haxeltine & Prentice, 1996) and the LPJ dynamic global vegetation model (Sitch *et al*., 2003), and representations of population dynamic processes as commonly adopted by forest gap models (Prentice *et al*., 1993).

Vegetation in LPJ-GUESS is represented as a mixture of plant functional types (PFTs), characterized by different structural, physiological, phenological and life-history attributes (Table 1). A limited set of bioclimatic parameters define the potential distribution of each PFT in climate space. The model simulates the growth of individual trees on a number of replicate patches, corresponding in size approximately to the area of influence of one large adult tree on its neighbors. Herbaceous vegetation is also represented, but individuals are not distinguished. Dynamic changes in indi-

Table 1 General characteristics distinguishing the five plant functional types (PFTs) used by LPJ-GUESS to simulate future impacts on European ecosystems

	Plant functional type				
	NE	TBS	IBS	TBE	G
Leaf phenology	Evergreen	Winter deciduous	Winter deciduous	Evergreen	Drought + winter deciduous
Shade tolerance	High	High	Low	High	Low
Fire tolerance	Low	Low	Low	Low	High
Minimun coldest month temperature (°C) for survival	No limit	−18	No limit	−7	No limit

NE, boreal/temperate needleleaved evergreen; TBS, temperate shade-tolerant broadleaved summergreen; IBS, boreal/temperate shade-intolerant broadleaved summergreen; TBE, temperate broadleaved evergreen; G, grass. For more detail about PFTs parameters see Smith *et al*. (2001).

vidual size and form influence the resource uptake and growth of neighbors. For the simulations performed in this study, each modeled individual plant corresponds to an average individual of a particular cohort (age class) of a PFT. Height and diameter growth are regulated by carbon allocation, conversion of sapwood to heartwood and a set of prescribed allometric relationships.

Physiological processes [e.g. photosynthesis, stomatal conductance, autotrophic and heterotrophic respiration (Rh)] and associated fluxes of carbon and water between soil layers, vegetation and the atmosphere are simulated on a daily time step. Growth of individual trees and grass populations, litterfall, fine root turnover, vegetation dynamics (including tree establishment and mortality) and disturbance are simulated on an annual time step. Environmental input data consist of temperature, precipitation, cloudiness or incoming shortwave radiation, atmospheric CO_2 concentrations and a soil texture class.

Carbon assimilation is calculated using a modified Farquhar's photosynthesis scheme (Haxeltine & Prentice, 1996). The amount of carbon fixed by an individual each year is influenced by temperature, atmospheric CO_2 concentration, absorbed photosynthetically active radiation (PAR) and stomatal conductance. PAR intercepted by vegetation is partitioned among individual trees according to the vertical distribution of their leaf area within the vegetation canopy and light extinction within the canopy. Carbon uptake by photosynthesis and water losses via transpiration are coupled through stomatal conductance (Haxeltine & Prentice, 1996). If the atmospheric demand for water exceeds the supply, determined by plant root-weighted soil moisture availability and maximum sapflow rates, then the stomatal conductance, which also limits CO_2 uptake for photosynthesis, is reduced until plant transpiration equals the supply. Soil moisture availability is simulated using a bucket model with two soil layers of fixed depth (0.5 m upper and 1 m lower; Haxeltine & Prentice, 1996) and percolation between layers. Evaporation from soil surfaces and rainfall interception by vegetation are also accounted for.

Three decomposable carbon pools that differ in their decomposition rates are distinguished in the model. The litter pool is assigned a decomposition rate of $0.35\,\text{year}^{-1}$ at 10 °C, while the intermediate and slow SOM pools are assigned decomposition rates of 0.03 and $0.001\,\text{year}^{-1}$, respectively, at 10 °C when soil moisture is at field capacity (Sitch *et al*., 2003). Decomposition rates are influenced by soil temperature through a modified Arrhenius relationship (Lloyd & Taylor, 1994) and increase with soil moisture (Foley *et al*., 1996).

LPJ-GUESS has been tested against observed terrestrial carbon and water fluxes and vegetation patterns in a number of studies (e.g. Smith *et al*., 2001; Hickler *et al*., 2004; Morales *et al*., 2005; Hély *et al*., 2006).

A full description of LPJ-GUESS is available in Smith *et al*. (2001). Further details of the physiological, biophysical and biogeochemical components of the model are given by Sitch *et al*. (2003). The version used in this study includes an improved representation of ecosystem water cycling as documented in Gerten *et al*. (2004).

Modeling protocol

Simulations of the ecosystem structure began from bare ground (no plant biomass present) and were then 'spun up' for 300 model years to achieve equilibrium in carbon pools sizes with respect to the long-term climate (i.e. a balance between ecosystem release and uptake of CO_2, averaged over a few years). A time series comprising the first 30 years of historical data (1901–1930; see next paragraph), detrended in the case of temperature, was used repeatedly as model input through the spin-up period. Equilibrium sizes of the two soil carbon pools were determined analytically, based on average litter inputs for the final years of the spin up.

The model was then driven using observed transient monthly data for the period 1901–1990 from the Climate Research Unit (CRU) $0.5 \times 0.5^\circ$ global historical climate dataset (New *et al*., 2000) and global atmospheric CO_2 concentrations from the Carbon Cycle Model Linkage project (McGuire *et al*., 2001).

Climate change impacts were assessed by comparing key characteristics of the ecosystems between a control period (1961–1990, taken from the above simulation forced by observations) and a future scenario period (2071–2100). This follows the classic approach for climate change impact analysis (e.g. Fowler *et al*., 2003; Payne *et al*., 2004). To model ecosystem behavior in the latter part of the 21st century, we used climate change scenarios provided by a range of RCM experiments from the PRUDENCE project. Each RCM is driven by data from one or more GCM simulations, and these describe both the baseline climate conditions for 1961–1990 and the climate under the SRES A2 or B2 emissions scenarios for 2071–2100; see also 'Climate models.'

However, as LPJ-GUESS must simulate ecosystem development for all years to 2100, it was necessary to fill the gap in the PRUDENCE data from 1991 to 2070. To achieve this, we first standardized the observed 1961–1990 climate data from the CRU dataset, by subtracting its 30-year means (computed for each calendar month) from each individual year and month, and then dividing by the 30-year standard deviations (SDs; again computed separately for each month). An 80-year time series of standardized data was then formed by repeat-

ing this 30-year standardized time series three times and removing the last 10 years. Finally, this was unstandardized to fill the gap period using time-evolving means and SDs that enable a smooth transition between the observed data at 1990 and the RCM scenario data at 2071. By 'unstandardize,' we mean to multiply by a time series of SDs and then add a time series of means. These time-evolving means and SDs were computed (separately for each calendar month) using linear trends of means and SDs between the RCM output for the control (1961–1990) and scenario (2071–2100) periods, and then rescaling these such that they matched the observed means and SDs for the period 1961–1990. In summary, the observed patterns of interannual variability were retained until 2070, but the temporal means and variances of the fields evolved smoothly and linearly between the two periods of climate data.

The atmospheric CO_2 concentrations in LPJ-GUESS for the scenario period 2071–2100 were taken as the estimates used in the PRUDENCE climate modeling experiments, which on average were 718 and 566 ppm for the A2 and B2 scenarios, respectively (Christensen *et al*., 2006). Potential changes in anthropogenic nitrogen deposition were neglected in this study: the impacts of increased nitrogen deposition, due to industrial and agricultural activity, are potentially relevant to the carbon exchange through changes in plant nutrient availability (Nadelhoffer *et al*., 1999), but are not yet included as a driver in LPJ-GUESS.

A 100-year mean disturbance interval, corresponding to average disturbance regimes for natural and managed forests in Europe, was implemented over the entire model domain and simulation period. Land use was taken into account by simulating separately, in each grid cell, potentially woody vegetation (forests and natural vegetation) and herbaceous vegetation (grasslands and croplands). The average PFT composition of the vegetation, its leaf area index (LAI), and carbon fluxes from vegetation and soils were then computed for each grid cell as the weighted average of the simulated values for the two vegetation classes, using observed present-day anthropogenic land cover data as weights. These data were derived from the PELCOM and CORINE databases (Mücher *et al*., 2000) within the ATEAM project (Schröter *et al*., 2005). We assumed that land cover up to and during the scenario period remains the same as at the present day.

Climate models

RCMs allow downscaling from the global scale of GCM simulations to regional scales. Generally, the GCM is used to provide a consistent representation of the large-scale global circulation, while the RCM is used to incorporate more detail to the climate simulations of temperature and precipitation as to the effect of regional features, such as topography and physiographic features (e.g. inland seas). In this study, we have used five RCMs that form part of a wider collection of downscaling experiments, conducted within the EU project PRUDENCE (Christensen *et al*., 2006):

(1) The SMHI Rossby Centre regional Atmosphere–Ocean model RCAO (Döscher *et al*., 2002).
(2) The HIRHAM RCM (Christensen *et al*., 1996) from the Danish Meteorological Institute.
(3) The CLM model (Steppeler *et al*., 2003) from GKSS.
(4) The UK Met Office Hadley Centre's HadRM3 H model (Buonomo *et al*., submitted).
(5) The REMO model of the Max-Planck Institute for Meteorology (Jacob, 2001).

We selected these experiments because they span the largest available geographical portion of Europe. They were driven by boundary conditions that were taken from two different GCMs, HadAM3H (Hudson & Jones, 2002) and ECHAM4/OPYC3 (Roeckner *et al*., 1999). They were integrated at a resolution of about 50 km, with a domain covering the European continent from the Mediterranean to Scandinavia and from Iceland to the Black Sea (Frei *et al*., 2006). The magnitude of the future changes in precipitation and temperature predicted by these RCMs depends not only on the boundary conditions used to force them but also on the specification of GHG forcing. In this study, the two emission scenarios used to force the RCMs are the IPCC SRES A2 anthropogenic emissions, representing rather high future GHG concentrations (836 ppm CO_2 at 2100), and B2, representing lower future emissions (611 ppm at 2100). Both scenarios are described thoroughly by Nakicenovic *et al*. (2000). The suite of predicted future climates used in this study to drive LPJ-GUESS is listed in Table 2.

Table 2 List of RCM-generated climate scenarios used, showing GCMs providing boundary conditions for the RCM downscaling and the driving IPCC SRES emissions scenarios

RCMs	GCM	Emissions scenarios
RCAO	HadAM3H	A2, B2
	ECHAM/OPYC	A2, B2
HIRHAM	HadAM3H	A2
	ECHAM/OPYC	A2, B2
HadRM3H	HadAM3H	A2
CLM	HadAM3H	A2
REMO	HadAM3H	A2

RCM, regional climate model; GCM, general circulation model.

Projected climate change

Future climatic changes over Europe are analyzed for five European subregions defined by Ruosteenoja *et al.* (2006; Fig. 1). The RCMs used in this study simulated increases in mean annual temperature, calculated as the difference between 2071–2100 and 1961–1990 averages for the whole of Europe, in a range from +3.5 to +6.0 °C (Table 3). Increases in annual precipitation for the European average range between 2.3% and 32.8% (Table 3).

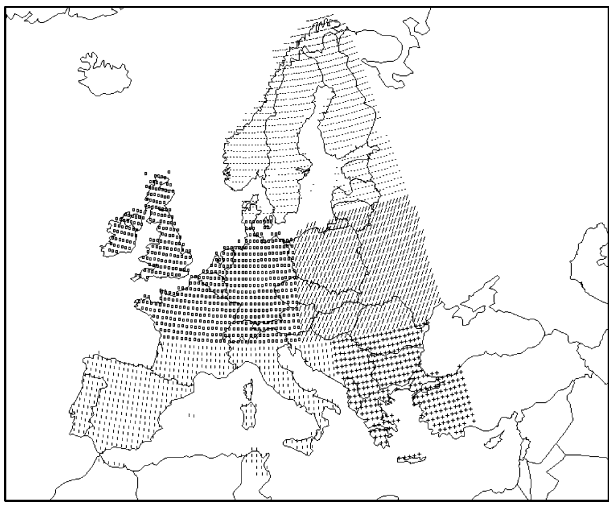

Fig. 1 Subregions over Europe. (–) N: 55–75°N, 4–35°E; (□) W: 45–55°N, 15°W–15°E and 55–65°N, 10°W–0°E; (/) E: 45–55°N, 15–35°E; (|) SW: 35–45°N, 15°W–18°E; (+) SE: 35–45°N, 18–35°E.

All models simulated an increase in average temperature over the five European subregions. The range for individual regions and models is between +2.3 °C simulated by CLM-HadAM3H-A2 in the SW subregion and +6.8 °C for the RCAO-ECHAM/OPYC-A2 scenario for the same subregion (Table 3). The latter scenario shows strong warming over the whole of Europe and the largest temperature increases among all the scenarios used in this study, while the CLM-HadAM3H-A2 scenario shows the smallest temperature changes. Comparing subregions, the smallest temperature increases generally apply to the E subregion (4.4 °C on average), while the strongest warming is in the W subregion (4.9 °C on average). Overall, for temperature, the relative spatial pattern projected by each RCM remains the same over different emission scenarios and different driving GCMs, and only the size of the anomaly varies between emission scenarios and driving GCMs (Table 3).

Table 3 Mean changes in temperature (°C) and precipitation (%) for 2071–2100 compared with 1961–1990 across five European subregions under the 10 RCM-generated climate scenarios used in the study

			European subregions					Total area
RCM/GCM	Emissions Scenario		SW	SE	E	W	N	average
RCAO/HadAM3H	A2	Δ temperature	4.9	5.4	5.0	6.0	4.8	5.0
		Δ precipitation	−22.9	−30.2	9.9	4.7	34.3	7.5
HIRHAM/HadAM3H	A2	Δ temperature	4.6	4.7	4.4	5.0	4.3	4.6
		Δ precipitation	−13.8	−20.4	5.6	0.1	16.6	2.3
CLM/HadAM3H	A2	Δ temperature	2.3	2.8	3.3	3.9	4.1	3.5
		Δ precipitation	−1.0	18.6	35.0	21.1	60.8	32.8
HadRM3H/HadAM3H	A2	Δ temperature	4.5	5.2	4.9	5.0	4.6	4.8
		Δ precipitation	−17.0	−19.3	10.0	0.1	28.6	5.8
REMO/HadAM3H	A2	Δ temperature	3.2	5.1	4.0	4.3	5.3	4.5
		Δ precipitation	−16.0	−5.8	20.2	11.9	50.4	19.8
RCAO/ECHAM/OPYC	A2	Δ temperature	6.8	6.4	6.1	6.3	5.4	6.0
		Δ precipitation	−38.3	−41.9	21.9	9.7	69.5	18.8
HIRHAM/ECHAM/OPYC	A2	Δ temperature	5.7	5.2	4.9	5.4	4.7	5.1
		Δ precipitation	−21.5	−9.0	15.0	15.3	40.2	14.0
RCAO/HadAM3H	B2	Δ temperature	3.6	4.1	3.6	3.9	3.7	3.7
		Δ precipitation	−15.1	−15.2	11.4	5.6	30.9	9.6
RCAO/ECHAM/OPYC	B2	Δ temperature	5.5	5.2	4.7	5.1	4.4	4.9
		Δ precipitation	−29.1	−26.8	34.1	46.8	61.6	23.0
HIRHAM/ECHAM/OPYC	B2	Δ temperature	4.4	3.9	3.6	4.2	3.8	3.9
		Δ precipitation	−14.4	−13.9	26.2	10.5	44.9	18.2
Mean		Δ temperature	4.6	4.8	4.4	4.9	4.5	
		Δ precipitation	−18.9	−16.4	18.9	12.6	43.8	

The sub-regions are shown in Fig. 1.
RCM, regional climate model.

Table 4 Mean changes in NPP (%) and Rh (%) for 2071–2100 compared with 1961–1990 across five European subregions simulated by LPJ-GUESS driven by the 10 RCM-generated climate scenarios

				European subregions				
RCM	GCM	Emissions scenario		SW	SE	E	W	N
RCAO	HadAM3H	A2	NPP	4.4	10.7	15.1	20.9	41.0
			Rh	10.2	17.9	19.3	26.7	43.2
HIRHAM	HadAM3H	A2	NPP	9.3	18.1	12.3	21.4	40.1
			Rh	14.4	24.9	19.0	25.8	44.7
CLM	HadAM3H	A2	NPP	12.1	22.0	22.1	28.6	44.1
			Rh	16.2	25.4	23.7	32.3	48.0
HadRM3H	HadAM3H	A2	NPP	5.3	13.3	11.0	19.7	46.1
			Rh	11.7	20.8	19.3	30.3	51.3
REMO	HadAM3H	A2	NPP	9.6	24.5	23.6	25.4	41.8
			Rh	15.9	30.8	27.7	27.8	47.3
RCAO	ECHAM/OPYC	A2	NPP	−7.6	8.5	4.9	11.2	36.0
			Rh	2.0	17.3	18.0	24.4	42.8
HIRHAM	ECHAM/OPYC	A2	NPP	5.8	13.2	8.7	17.4	40.2
			Rh	12.8	21.5	19.0	25.5	46.3
RCAO	HadAM3H	B2	NPP	2.6	12.0	13.0	14.7	28.2
			Rh	8.0	18.3	16.9	18.3	33.3
RCAO	ECHAM/OPYC	B2	NPP	−1.4	12.6	8.7	13.0	27.7
			Rh	6.1	19.0	16.0	24.4	35.7
HIRHAM	ECHAM/OPYC	B2	NPP	5.7	14.1	8.9	16.6	33.3
			Rh	11.5	21.8	16.6	21.4	39.5
Mean			NPP	4.6	14.9	12.8	18.9	37.9
			Rh	10.9	21.8	19.6	25.7	43.2
Standard deviation			NPP	5.4	4.8	5.7	5.2	6.0
			Rh	4.3	4.0	3.4	3.8	5.3

The sub-regions are shown in Fig. 1.
RCM, regional climate model; GCM, general circulation model; NPP, net primary production; Rh, heterotrophic respiration.

With regard to precipitation, there are major differences among the climate model combinations in terms of the projected changes. Overall, all scenarios describe increases in annual precipitation when averaged over the whole of Europe, but the regional patterns differ greatly (Table 3). A general decrease is predicted in Mediterranean areas (i.e. SW and SE subregions), and a relatively large increase in precipitation in the N subregion, while in the temperate area (i.e. subregions E and W), changes tend to be moderate (Table 3). CLM-HadAM3H-A2 describes the largest increase in precipitation averaged across the whole of Europe, while HIRHAM-HadAM3H-A2 and HadRM3H-HadAM3H-A2 describe the smallest changes. The sign of the projected precipitation trend is more dependent on the GCM and region than on the RCM (Table 3).

Results

We analyzed modeled changes in carbon fluxes and stocks as the difference between averages for the 30-year time slices 1961–1990 and 2071–2100. NPP, the net assimilation of CO_2 into organic matter by plants, represents the rate of carbon input into terrestrial ecosystems (Cao & Woodward, 1998). Annual NEE represents the net exchange of carbon between terrestrial ecosystems and the atmosphere and corresponds to the difference between NPP and Rh. When reporting values of NEE, we follow the IPCC convention that a negative value represents a net flux of CO_2 from the atmosphere to the ecosystem (i.e. a carbon sink), while positive values represent a flux to the atmosphere (i.e. a carbon source). Results are presented both for the five European subregions presented in Fig. 1 and as averages for Europe as a whole.

NPP

Simulations of present day (1961–1990) NPP by LPJ-GUESS, using historical climate data, reached on average 0.38 $kg\,C\,m^{-2}\,yr^{-1}$, which compares well with other

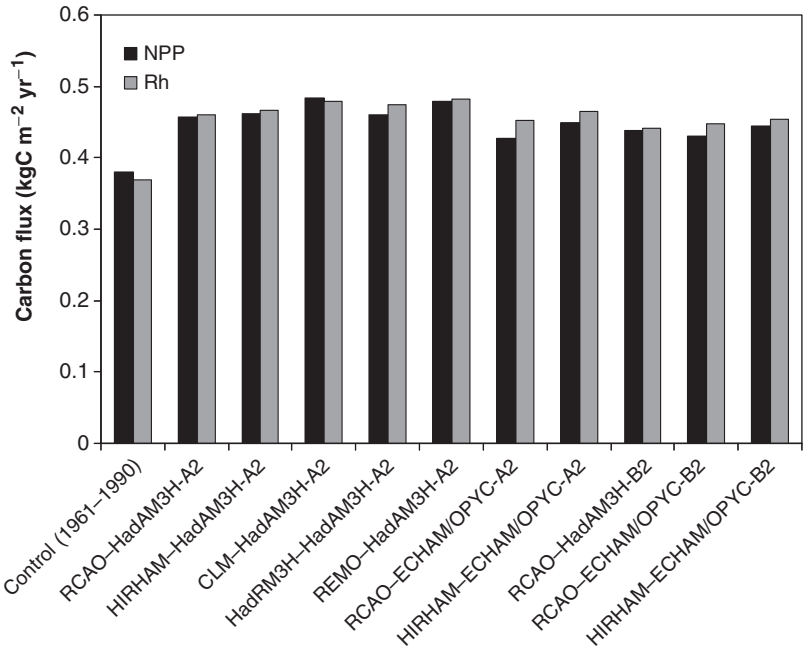

Fig. 2 Mean net primary production (NPP) and heterotrophic respiration (Rh) averaged over Europe for the period 2071–2100, simulated by LPJ-GUESS driven by the 10 regional climate model-generated climate scenarios. Results of the control simulation (1961–1990) are shown for comparison.

estimates for Europe (Cramer *et al*., 1999; Kucharik *et al*., 2000).

Averaged among scenarios, the NPP predicted by LPJ-GUESS increased for Europe as a whole (Table 4; Figs 2 and 3). These increases were primarily the result of the physiological and phenological effects of higher temperatures and fertilization effects of increased CO_2 levels (Ainsworth & Long, 2005). Consequences for NPP of changes in precipitation and feedbacks of vegetation changes, such as replacement of boreal conifers by broadleaved trees (Table 5), were of secondary importance. In general, the A2 scenarios were associated with slightly larger changes in NPP than B2 scenarios (Table 4; Figs 2 and 3), both because the emissions-driven climatic changes were generally greater, and because of the stronger effects of higher atmospheric CO_2 levels on plant physiology in the A2 scenario. In some southern areas, however, increased evapotranspiration and soil water depletion offset the positive effect of the higher CO_2 concentrations on NPP. This effect was generally more pronounced in the A2 scenarios (Table 4; Fig. 3).

Comparing scenarios differing in the GCM providing boundary conditions for the RCM simulations, HadAM3H-based scenarios generally resulted in larger increases in NPP over Europe compared with the ECHAM–OPYC-based scenarios (Table 4; Figs 2 and 3).

The greatest proportional changes in NPP were predicted to occur in the N subregion, while the smallest changes were predicted for SW Europe (Table 4), and this was consistent across all RCM scenarios (Table 4; Fig. 3). Net changes in SE Europe were positive, but modest compared with the northerly subregions. NPP decreases in southern areas were caused primarily by marked reductions in precipitation (Table 3), which together with warming-driven increases in evapotranspiration led to soil water deficits and reduced plant productivity.

Heterotrophic respiration

Rh was predicted to increase throughout Europe in all simulations because of the warmer future described by the RCM scenarios, although there were substantial differences in the magnitude of this increase among subregions and RCM scenarios (Table 4). Changes in Rh broadly reflect changes in NPP, because the latter controls the amount of litter produced through mortality and tissue turnover (e.g. leaf shedding), as the major pathway of carbon transfer to the heterotroph community (Fig. 2). Marginal differences between changes in NPP and Rh depend on the size of the existing pool of recalcitrant soil carbon (which continues to decay for decades to centuries following a change in conditions)

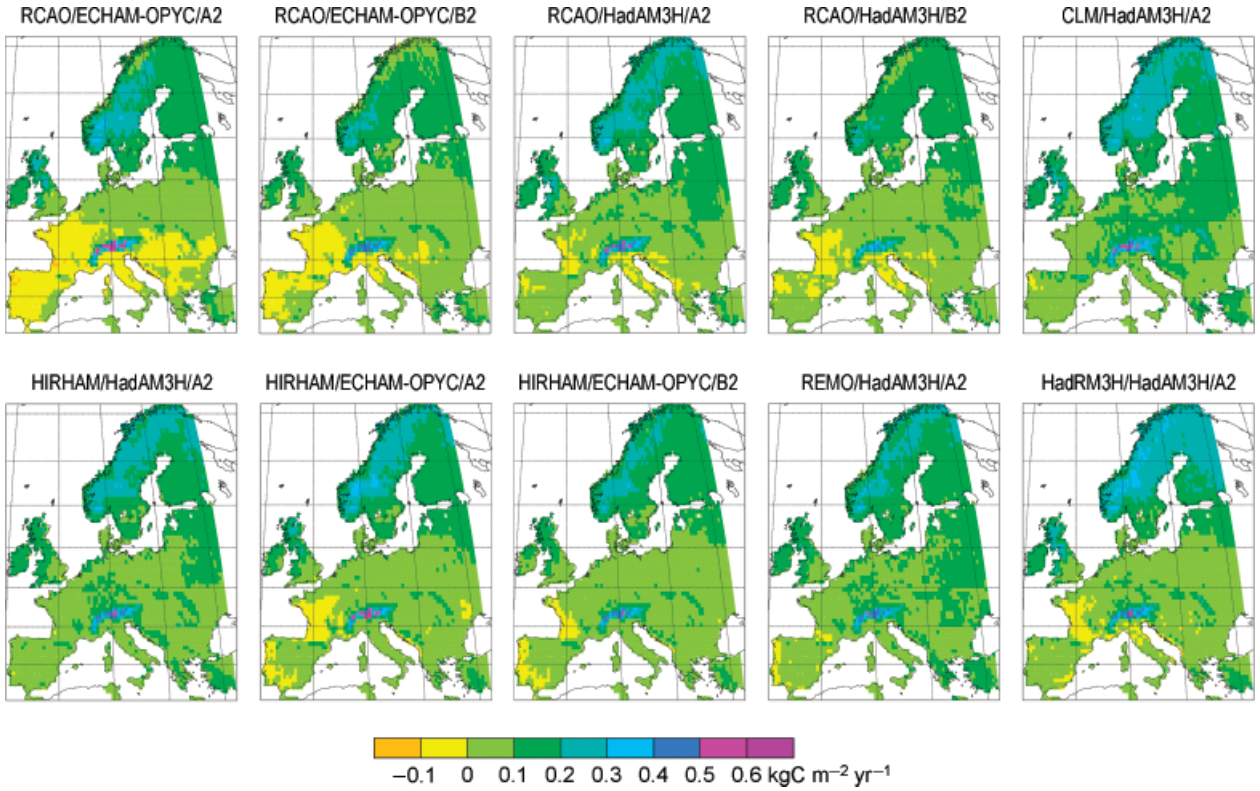

Fig. 3 Net primary production changes by 2071–2100 compared with the control period (1961–1990) simulated by LPJ-GUESS under the 10 regional climate model-generated climate scenarios.

Table 5 Leaf area index of dominant PFTs at the Boreal (N sub-region) and Mediterranean (SW and SE subregions) zones in Europe. Results are presented for control period (1961–1990) and the four future climate scenarios generated by RCAO

Subregions	PFT	Control (1961–1990)	RCAO H-A2	RCAO H-B2	RCAO E-A2	RCAO E-B2
N (Boreal)	NE	1.1	1.3	1.2	1.2	1.2
	TBS	0.2	0.7	0.5	0.7	0.6
	IBS	0.7	1.1	0.9	1.1	1.0
	G	0.9	0.9	0.9	0.8	0.8
SW and SE (Mediterranean)	TBE	0.4	0.7	0.6	0.7	0.7
	TBS	0.4	0.4	0.4	0.3	0.4
	NE	0.1	0.1	0.1	0.1	0.1
	IBS	0.4	0.4	0.4	0.3	0.4
	G	1.9	2.0	2.0	1.9	1.9

PFTs are listed in Table 1.
PFT, plant functional type.

and on the adjustment in respiration rate per unit carbon, which is sensitive to soil temperatures and moisture. For example, in the N subregion, proportional increases in Rh and NPP were similar, but in the southern subregions, Rh increased more strongly (Table 4), reflecting temperature increases on top of a higher baseline temperature compared with northern and central areas. Simulated changes in Rh were consistently higher under the A2 scenarios compared with the B2 scenarios, mainly reflecting the greater amplitude of temperature changes (Table 4; Fig. 2).

Annual and spatial variability of NEE and cumulative carbon stocks in Europe

Averaged across scenarios, European ecosystems exhibited a small net carbon sequestration (negative NEE)

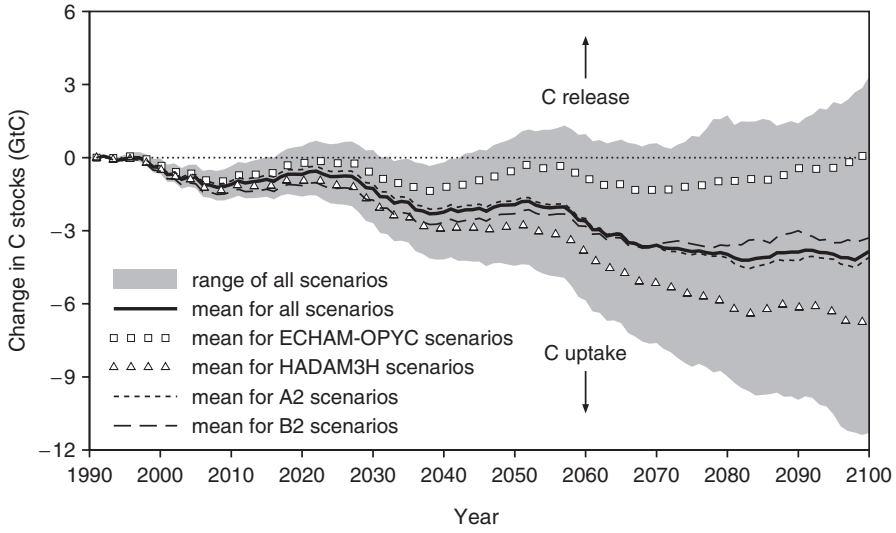

Fig. 4 Cumulative change in ecosystem carbon stocks averaged over Europe simulated by LPJ-GUESS under the 10 regional climate model-generated climate scenarios, showing average trajectories for the ECHAM/OPYC-based scenarios, HadAM3H-based scenarios, A2 emissions-based scenarios, B2 emissions-based scenarios and the overall average. The gray area shows the range among all scenarios. Negative values represent an uptake of carbon by terrestrial ecosystems.

until 2070, followed by a carbon-neutral behavior or a net release until the end of the scenario period, although with considerable variation among years and scenarios (Fig. 4). The predicted average carbon sink by the year 2100 was 3.8 Gt C, but the climate scenario-dependent uncertainty is large, ranging from a sink of 11.6 Gt C to a source to the atmosphere of about 3.3 Gt C (Fig. 4). The intervening period (1991–2070) exhibited some weak decadal-scale cyclicity between periods of overall carbon uptake (e.g. around 2030) and release (e.g. around 2060); however, it should be noted that this variability mainly reflects a repeating pattern in the artificially constructed climate data series bridging the gap between the observed climate of the control period and the RCM-generated scenarios (see 'Climate models').

Differences between GCMs (ECHAM–OPYC vs. HadAM3H) were much more important than differences between RCMs or between emissions scenarios (A2 vs. B2), in terms of the consequences of the associated climate scenarios on the projected development of ecosystem carbon stocks (Fig. 4). RCMs driven by ECHAM–OPYC showed, on average, no carbon sink by the end of the scenario period, while HadAM3H-driven RCMs showed an average accumulated carbon uptake of 6.7 Gt C by 2100.

Figure 5 shows the geographic variation in simulated NEE for the control period (1961–1990) and for the suite of scenarios generated by the RCAO and HIRHAM RCMs. During the control period, most northern-European ecosystems, most of Italy, and parts of the Balkan behaved as a sink of carbon, while some areas of Central and Western Europe released small amounts of carbon, with the rest of Europe exhibiting an approximate equilibrium between the uptake of carbon and its release to the atmosphere.

Under the scenario period (2071–2100), most areas in central Europe (E and W subregions) switched from sinks to sources of carbon according to the model (Fig. 5). The additional carbon losses tended to be more pronounced in the case of the scenarios based on the ECHAM–OPYC GCM, compared with the HadAM3H GCM, and for A2 compared with B2 emissions. Terrestrial ecosystems in northern latitudes and the Alps generally increased in sink strength. At the highest altitudes, vegetation colonized previously barren areas rendered accessible by climatic amelioration, while trees advanced onto alpine grassland or tundra, in both cases inducing a transient accumulation of carbon. These spatial patterns, and also the magnitudes of the projected NEE fluxes, were relatively similar under the corresponding RCAO- and HIRHAM-generated scenarios.

Discussion

Overall patterns among scenarios

The model simulated NPP increases over almost all of Europe for both emission scenarios which were primarily caused by higher temperatures, a longer growing

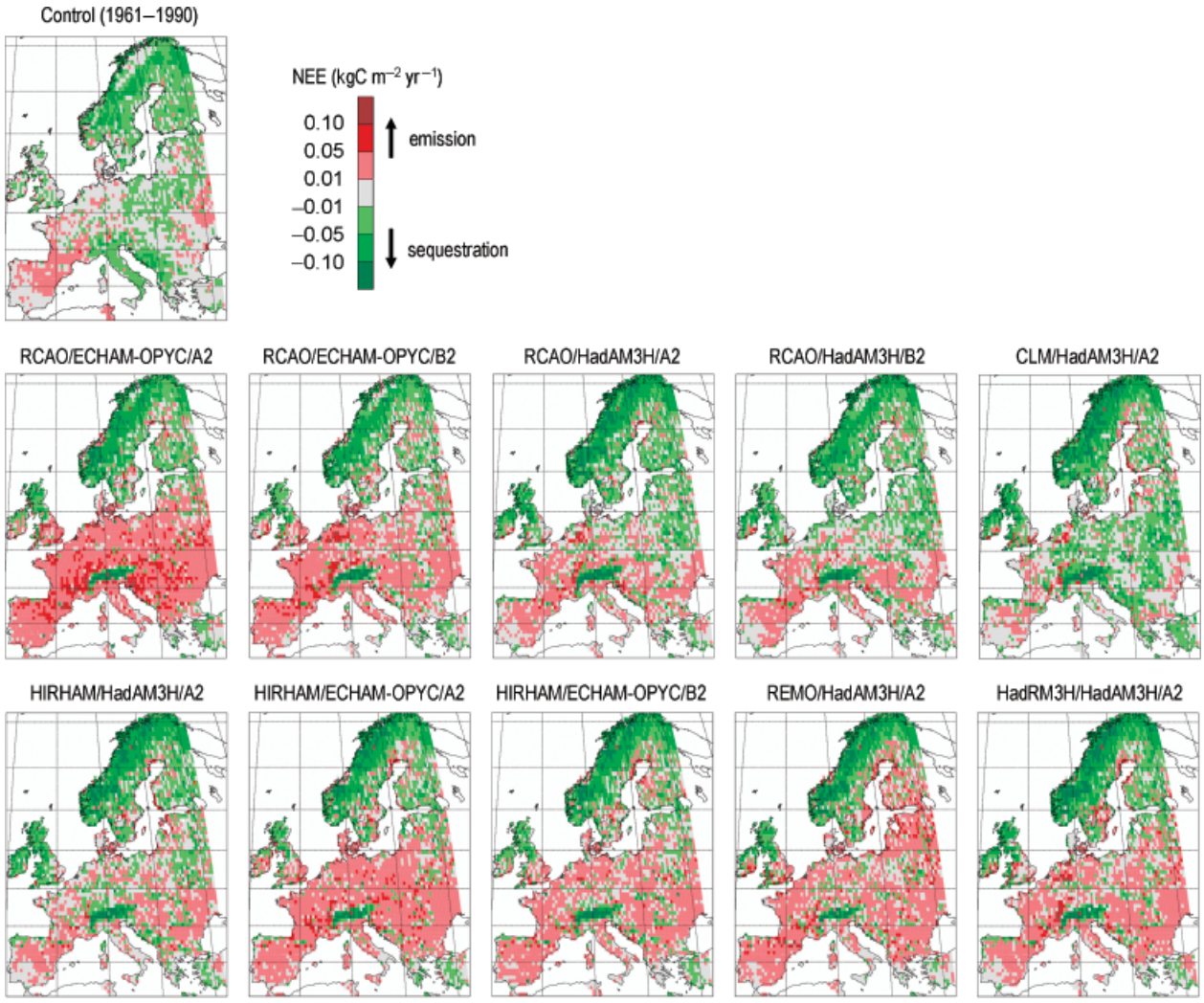

Fig. 5 Net ecosystem carbon exchange (NEE) for the scenario period 2071–2100 simulated by LPJ-GUESS under the 10 regional climate model-generated climate scenarios. Results for the control period 1961–1990 are included for comparison. Negative values represent an uptake of carbon by terrestrial ecosystems.

season in the north and at high altitudes, and physiological effects of rising CO_2 concentrations in the atmosphere. Vegetation growth is limited by a short growing season, particularly in northern Europe. Higher average temperatures advance the onset of vegetation activity in the spring and extend the active phase in the autumn, enhancing productivity on an annual basis (Kimball *et al*., 2004). Higher temperatures also have the potential to accelerate net photosynthesis, especially during the early growing season in colder climates (Jarvis & Linder, 2000; Tanja *et al*., 2003). Increased CO_2 concentrations enhance the efficiency of photosynthesis and water use (Ainsworth & Long, 2005). In terms of vegetation production, the overall picture described for Europe is of a continuation of the trend, already seen in multidecadal satellite data records, of increased 'greening' associated with longer growing seasons and increased vegetation productivity (Myneni *et al*., 1997; Lucht *et al*., 2002).

Regional patterns of NPP for the scenario period 2071–2100 were relatively robust across scenarios generated by different RCMs. NPP enhancement was strongest and most consistent in the N subregion, where increasing temperatures resulted in significant growing-season extension. Positive growth trends associated with warming have already been documented for boreal forests (Kimball *et al*., 2004) and the modeled changes are consistent with observations and understanding of climate effects on boreal forests (Myneni *et al*., 1997; Liski *et al*., 2003). The model also predicted changes in vegetation composition and distribution, including dominance shifts from conifers to deciduous trees, and tree-line advance in the Fennoscandian mountain range and the Alps. Coniferous forests gen-

erally remained the dominant forest type of the boreal zone, but the increase in LAI between the control and scenario period was modest (between 13% and 19%) for coniferous forest in comparison with the increase in deciduous forest (between 40% and 60%; Table 5). Using an equilibrium bioclimatic model (STASH) Sykes & Prentice (1996) likewise predicted an expansion of coniferous forest (Norway spruce and Scots pine) into extant tundra regions under a doubled-CO_2 scenario. These changes were predicted to be accompanied by a northward shift in the southern limits of these two species in Fennoscandia. In the present study, population processes (lagging of mortality relative to recruitment) allowed boreal trees to remain present in declining abundance as the climatological regeneration niche migrates northwards. This arguably provides a more realistic description of the transient vegetation dynamics that may be expected to occur through to the late 21st century (Malanson & Cairns, 1997).

Results for the N subregion suggest that the enhanced productivity might in part become balanced by increasing carbon losses through respiration resulting from a combined effect of higher temperatures and increased precipitation. Increased decomposition rates as a result of increased temperatures have been demonstrated experimentally in a number of studies in boreal vegetation (Johansson, 1994; Johansson *et al*., 1995).

The smaller increase, or decrease, in NPP projected for southern Europe in comparison with more northerly areas was mainly determined by water limitations and their effects on vegetation. Reductions in precipitation were projected for both the SW and SE subregions under nearly all scenarios, while temperature increases were comparable with more northerly regions and would tend to lead to soil moisture depletion by evapotranspiration (Table 3). This negative effect of decreasing soil moisture on NPP can, however, be partly offset by decreased stomatal conductance, a common physiological response to elevated CO_2 (Gerten *et al*., 2005). In LPJ-GUESS, the net effect depends on the balance between a negative effect of elevated CO_2 on canopy conductance on the one hand, and increasing photosynthesis, leaf area and atmospheric demand for water under climate change, which increase water losses through transpiration (Gerten *et al*., 2005), on the other hand. In common with much of the northern hemisphere temperate zone, southern European ecosystems have exhibited a positive growth trend in recent decades (Nemani *et al*., 2003). Results of the present study suggest that this trend might continue or reverse before the end of the 21st century, depending on the magnitude of warming and precipitation changes, and their net effect on water balance.

LPJ-GUESS simulated, on average, increases in Rh across all European subregions for the scenario period and these increases also showed clear regional patterns (Table 4). Although increased NPP is not automatically reflected in increased plant biomass in the model, additional carbon is expected to enter the soil by enhanced litter production from roots and leaves. In addition, litter production could be temporarily enhanced by mortality events; for example, in association with drought stress, or in PFT populations stranded outside their climatic niche as isotherms migrate northwards. Changes in Rh predicted in this study are in agreement with field studies that have indicated increases in soil organic matter, and increases in soil respiration under elevated CO_2 (Schlesinger & Andrews, 2000).

Our analyses reveal large uncertainty in future estimates of the carbon balance of European terrestrial ecosystems that is related to the climate predictions (Fig. 4). The predicted changes in the carbon balance of European terrestrial ecosystems are, however, minor in comparison with GHG emissions: the average cumulative carbon sink [3.8 Gt C in total, or 0.035 Gt C per year until 2100 (Fig. 4)] represents 1.85% of the current EU GHG emission rate of ca. 1.87 Gt C yr^{-1} (Janssens *et al*., 2003). When considering the whole range of simulations (Fig. 4), the maximum carbon release (3.3 Gt C) represents 1.6%, while the maximum uptake (11.6 Gt C) would amount to a sequestration of 5.6% of anthropogenic emissions. In another recent study, the carbon sequestration potential of European terrestrial ecosystems was projected to range from 1.8 to 4.9 Gt C over the period 1990–2080 (Schröter *et al*., 2005), based on GCM-generated climate scenarios spanning a number of GCMs and emissions levels. The latter study was confined to the 15 pre-2004 EU member states along with Norway and Switzerland, and thus excluded a number of central-eastern European countries whose ecosystems tend to be net carbon sources by the late 21st century, according to the simulations of the present study (Fig. 5). While this difference in geographical domain might account for the larger range among projections of the ecosystem carbon balance in the present study, it remains possible that other factors, such as differences in climate scenarios or in ecosystem model sensitivity to climate and CO_2 forcing, may also have played a role.

Uncertainties in modeled carbon fluxes

Uncertainties associated with driving scenarios. The driving environmental data constitute one important source of uncertainty when modeling the terrestrial biosphere (Knorr & Heimann, 2001). A chain of uncertainty

propagates from the emission scenarios and their underlying assumptions to uncertainties in climate processes, as well as errors arising from the spatial representation of global physiography in GCMs, to process and spatial uncertainties in RCMs.

RCMs provide an increase in resolution and can capture physical processes and feedbacks occurring at the regional scale, but they inherit the errors of the GCM providing boundary conditions for the RCM simulation. In addition, RCMs are unable to take account of feedbacks of regional changes – for example, in land surface energy balance – on global climate forcing (NRC, 2001). Current RCMs also lack dynamic vegetation or carbon cycling, so are unable to take account of feedbacks related to the evolution of vegetation structure, composition and growth as conditions change. The effects of regional-to-global feedbacks are highly relevant when assessing the carbon cycle and GHG forcing and can be a significant source of uncertainty (IPCC, 2001).

The type of GCM chosen to drive the RCM can have a large effect on predicted impacts as has been demonstrated by this study. The sensitivity of RCM-generated temperatures and precipitation levels to the driving GCM was investigated by Déqué *et al*. (2006) and Rowell (2006). Overall, differences between GCMs seem to be more important than differences between RCMs in determining the projected climate and its consequences for ecosystem carbon exchange and stocks (Figs 4 and 5). In contrast to the HadAM3H-based scenarios, the higher temperatures described by the ECHAM–OPYC-based scenarios led to weaker overall sinks and a net release of carbon from ecosystems to the atmosphere by the late 21st century, according to our simulations. When driven by ECHAM–OPYC climate data, the RCMs tended to predict strong precipitation decreases in some parts of southern Europe. According to LPJ-GUESS, this led to weaker positive or negative productivity changes while at the same time, rising temperatures stimulated soil respiration, resulting in net carbon losses from ecosystems.

Our results showed that the choice of the emissions scenario influences NPP and subsequently the evolution of future carbon stocks. Overall, simulations based on the A2 scenario had higher predicted NPP compared with the B2-based scenarios (Table 4). In terms of overall changes in carbon storage in Europe, however, the choice of emissions scenario was not important (Fig. 4). While the higher atmospheric CO_2 concentrations under the A2 scenario would tend to augment production in the model, the generally stronger forcing of precipitation and temperatures in this scenario tended to suppress production in some southern areas via increased drought stress, and higher temperatures led to increased soil respiration so that overall trends for Europe remained similar to B2. Previous studies employing DGVMs likewise point to an important role of rising atmospheric CO_2 concentrations for long-term trends in vegetation productivity (Bachelet *et al*., 2003; Sitch *et al*., 2003; Schaphoff *et al*., 2006). It should be noted, however, that these studies, like the present one, did not take account of the potential for negative biogeochemical feedbacks to reduce the carbon fertilization effects on longer time scales (Hungate *et al*., 2003; see also next subsection).

Uncertainties associated with the ecosystem model. LPJ-GUESS and the closely related global model LPJ-DGVM have been shown to reproduce broad general patterns of carbon exchange and vegetation dynamics at different scales. LPJ-GUESS and other process-based models have been benchmarked against eddy flux measurements at EUROFLUX forest sites throughout Europe, and shown to produce acceptable fits to seasonal carbon and water fluxes (Morales *et al*., 2005). Performance tended to be poorer at Mediterranean sites, with representations of the mechanisms of response of plant physiology and allocation, and of microbial activity, to soil water deficits being identified as possible causes of model-data mismatches. Negative feedbacks of soil water deficits on production, as well as temperature-driven increases in soil respiration, were important for overall patterns of change in the carbon balance of European ecosystems in the simulations of the present study. Given the known uncertainties in the ecosystem model, the details of the simulated responses, especially in southern Europe, should be interpreted with caution.

Zaehle *et al*. (2005) assessed the potential importance of parameter-based uncertainty for projections of carbon accumulation in vegetation and the turnover time of SOM under present and future climate in the global model LPJ-DGVM. Uncertainty as to the 'correct' values of 36 parameters in the model was found to propagate to an uncertainty range of $-3.35 \pm 1.45\,\mathrm{Gt\,C\,yr^{-1}}$ for global land-atmosphere fluxes under a climate and CO_2 scenario for the late 21st century. Most of the uncertainty propagated from parameters controlling photosynthesis, plant respiration and plant water balance. Uncertainty derived from parameter values in the ecosystem model was not quantified in the present study. However, it must be assumed that this class of uncertainty in LPJ-GUESS – which shares the same formulations of physiological, biophysical and biogeochemical processes with the global model employed in the Zaehle study – is potentially large, and would further extend the range of plausible futures, for example with regard to net carbon exchange by ecosystems in Europe (cf. Fig. 4).

As noted above, the CO_2 fertilization effect played an important role in the magnitude of simulated changes in

NPP and NEE, and for differences among scenarios. LPJ-GUESS has been shown to reproduce the observed enhancement of NPP in response to elevated CO_2 in a number of forest Free Air CO_2 Enrichment (FACE) experiments (Gerten *et al.*, 2005). However, it is believed that negative biogeochemical feedbacks and nutrient (particularly nitrogen) limitations may counteract CO_2 fertilization on time scales of decades or more (Hungate *et al.*, 2003). These factors are not accounted for in LPJ-GUESS. Longer experimental time series and better process understanding will be necessary to improve the representation of long-term responses to elevated CO_2 in large-scale ecosystem models.

Uncertainties related to land use change and forest management. The simulations performed in this study assume that present-day anthropogenic land use patterns remain constant to the end of the 21st century. In reality, impacts of climate change on carbon fluxes at the regional scale will likely be moderated by changes in land use. In Europe, improvements in technology might, for example, lead to replacement of agricultural land by forest (Rounsevell *et al.*, 2003), amplifying the increase in forest growing stocks simulated in response to climate and CO_2 changes alone. The present study does not take into account the effects of forest management on carbon stocks and net carbon sequestration. Several studies have shown that carbon stored in tree biomass and soils can be increased by adaptive management, with potentially large effects on carbon sequestration (Liski *et al.*, 2001; Masera *et al.*, 2003; Nabuurs *et al.*, 2003).

Conclusions

Our results suggest that European terrestrial ecosystem NPP might increase considerably under climate change. As carbon losses from Rh also are likely to increase, the net effect on the carbon balance will most probably be small compared with European GHG emissions, our results showing an average carbon uptake corresponding to 1.85% of present-day emissions. We identified considerable climate model and emissions-based uncertainty in these estimates, with the projected cumulative carbon exchange between terrestrial ecosystems and the atmosphere over the period 1991–2100 ranging from a sink of 11.6 Gt C to a source of 3.3 Gt C. Ecosystem model uncertainties were not quantified, but would be expected to extend this range.

The results showed a clear discrepancy in ecosystem impacts between southern and northern areas of Europe. In southern Europe, ecosystem impacts will likely be dominated by the effects of increasing growing season water deficits, whereas impacts in northern Europe are dominated by changes in the duration of the growing season and the efficiency of carbon assimilation.

The choice of GCM providing boundary conditions for the RCM was shown to be more important than the differences between RCMs in terms of effect of the generated climate scenarios on ecosystem properties, as simulated by our model. The warmer and – in southern areas – drier future described by the EC-HAM–OPYC-based scenarios was associated with a smaller cumulative sink of carbon to European ecosystems, compared with the HadAM3H-based scenarios.

The simulations have demonstrated the importance of using a suite of climate scenarios when assessing potential future changes in ecosystem properties. The magnitude of the GCM-, RCM- and emissions-based uncertainties in future impacts revealed by this study underlines the fact that modeled future carbon fluxes should be taken as characterizations of possible outcomes, rather than predictions.

We believe that this work is a relevant contribution to the understanding of the vulnerability of European ecosystems to global change, as well as their potential to mitigate greenhouse forcing in the longer term. In spite of quantitative differences, the ecosystem impacts of the range of scenarios considered are qualitatively robust both in space and time. Qualitative features of our results – such as the contrast in responses of northern and southern European ecosystems – can be employed with some confidence as a basis for policy-making. Our results should also provide guidance for climate modelers on the types of climate scenarios required for impact analyses using ecosystem models.

Acknowledgements

We thank two anonymous referees for thoughtful comments, which improved the manuscript. This study was funded by PRUDENCE (Contract EVK2-CT2001-00132) project in the EU fifth Framework program for Energy, environment, and sustainable development. The PRUDENCE RCM scenarios were provided by the participating regional climate modeling groups in the project. Ben Smith acknowledges financial support from the Swedish Research Council for Agricultural Sciences, Environment and Spatial Planning. David Rowell was partly supported by the UK Department for Environment, Food and Rural Affairs under contract PECD 7/12/37.

References

Ainsworth EA, Long SP (2005) What have we learned from 15 years of free-air CO_2 enrichment (FACE)? A meta-analytic review of the responses of photosynthesis, canopy properties and plant production to rising CO_2. *New Phytologist*, **165**, 351–372.

Arnell NW (2004) Climate change and global water resources: SRES emissions and socio-economic scenarios. *Global Environmental Change*, **14**, 31–52.

Bachelet D, Neilson RP, Hickler T *et al*. (2003) Simulating past and future dynamics of natural ecosystems in the United States. *Global Biogeochemical Cycles*, **17**, 1045.

Buonomo E, Jones RG, Huntingford C *et al*. (submitted) The robustness of high resolution projections of changes in extreme rainfall for Europe. *Quarterly Journal of the Royal Meteorological Society*.

Cao MK, Woodward FI (1998) Net primary and ecosystem production and carbon stocks of terrestrial ecosystems and their response to climatic change. *Global Change Biology*, **4**, 185–198.

Christensen JH, Carter TR, Rummukainen M (2006) Evaluating the performance and utility of regional climate models in climate change research: reducing uncertainties in climate change projections – the PRUDENCE approach. *Climatic Change*, in press.

Christensen JH, Christensen OB, Lopez P *et al*. (1996) *The HIRHAM4 Regional Atmospheric Climate Model. DMI Science Report 96–4*. Danish Meteorological Institute, Copenhagen, Denmark.

Conference of the Parties. (1998) *Kyoto Protocol to the United Nations Framework Convention on Climate Change. Report of the Conference of the Parties, Third Session Kyoto*. United Nations, Bonn, Germany.

Cramer W, Bondeau A, Woodward FI *et al*. (2001) Global response of terrestrial ecosystem structure and function to CO_2 and climate change: results from six dynamic global vegetation models. *Global Change Biology*, **7**, 357–373.

Cramer W, Kicklighter DW, Bondeau A *et al*. (1999) Comparing global models of terrestrial net primary productivity (NPP): overview and key results. *Global Change Biology*, **5** (Suppl. 1), 1–15.

Déqué M, Rowell DP, Luthi D *et al*. (2006) An intercomparison of regional climate simulations for Europe: assessing uncertainties in model projections. *Climatic Change*, in press.

Döscher R, Willén U, Jones C *et al*. (2002) The development of the coupled regional ocean-atmosphere model RCAO. *Boreal Environmental Research*, **7**, 183–192.

Foley JA, Prentice IC, Ramankutty N *et al*. (1996) An integrated biosphere model of land surface processes, terrestrial carbon balance, and vegetation dynamics. *Global Biogeochemical Cycles*, **10**, 603–628.

Fowler HJ, Kilsby CG, O'Connell PE (2003) Modeling the impacts of climatic change and variability on the reliability, resilience and vulnerability of a water resource system. *Water Resources Research*, **39**, 1222.

Frei C, Schöll R, Fukutome S *et al*. (2006) Future change of precipitation extremes in Europe: an intercomparison of scenarios from regional climate models. *Journal of Geophysical Research*, **111**, DO6105, doi: 10.1029/2005JD005965.

Gerten D, Lucht W, Schaphoff S *et al*. (2005) Hydrologic resilience of the terrestrial biosphere. *Geophysical Research Letters*, **32**, L21408.

Gerten D, Schaphoff S, Haberlandt U *et al*. (2004) Terrestrial vegetation and water balance – hydrological evaluation of a dynamic global vegetation model. *Journal of Hydrology*, **286**, 249–270.

Haxeltine A, Prentice IC (1996) BIOME3: an equilibrium terrestrial biosphere model based on ecophysiological constraints, resource availability and competition among plant functional types. *Global Biogeochemical Cycles*, **10**, 693–710.

Hély C, Bremond L, Alleaume S *et al*. (2006) Sensitivity of African biomes to changes in the precipitation regime. *Global Ecology and Biogeography*, **15**, 258–270.

Hickler T, Smith B, Sykes MT *et al*. (2004) Using a generalized vegetation model to simulate vegetation dynamics in northeastern USA. *Ecology*, **85**, 519–530.

Houghton RA, Davidson EA, Woodwell GM (1998) Missing sinks, feedbacks, and understanding the role of terrestrial ecosystems in the global carbon balance. *Global Biogeochemistry and Cycles*, **12**, 25–34.

Hudson DA, Jones RG (2002) *Simulations of Present-Day and Future Climate Over Southern Africa using HadAM3H. Hadley Centre Technical Note 39*. Hadley Centre for Climate Prediction and Research, Met Office, Bracknell, UK.

Hungate BA, Dukes JS, Shaw MR *et al*. (2003) Nitrogen and climate change. *Science*, **302**, 1512–1513.

IPCC (2001) *Climate Change 2001: The Scientific Basis*. Cambridge University Press, Cambridge.

Jacob D (2001) A note to the simulation of the annual and interannual variability of the water budget over the Baltic Sea drainage basin. *Meteorology and Atmospheric Physics*, **77**, 61–73.

Janssens IA, Freibauer A, Ciais P *et al*. (2003) Europe's terrestrial biosphere absorbs 7 to 12% of European anthropogenic CO_2 emissions. *Science*, **300**, 1538–1542.

Jarvis P, Linder S (2000) Constraints to growth of boreal forests. *Nature*, **405**, 904–905.

Jha M, Pan Z, Takle ES *et al*. (2004) Impacts of climate change on stream flow in the upper Mississippi river basin: a regional climate model perspective. *Journal of Geophysical Research*, **109**, D09105.

Johansson M-B (1994) Decomposition rates of Scots pine needle litter related to site properties, litter quality, and climate. *Canadian Journal of Forest Research*, **24**, 1771–1781.

Johansson M-B, Berg B, Meentemeyer V (1995) Litter mass-loss rates in late stages of decomposition in a climatic transect of pine forests: long-term decomposition in a Scots pine forest. *Canadian Journal of Botany*, **73**, 1509–1521.

Kimball J, McDonald KC, Running SW *et al*. (2004) Satellite radar remote sensing of seasonal growing seasons for boreal and sub-alpine evergreen forests. *Remote Sensing of Environment*, **90**, 243–258.

Knorr W, Heimann M (2001) Uncertainties in global terrestrial biosphere modelling: 1. A comprehensive sensitivity analysis with a new photosynthesis and energy balance scheme. *Global Biogeochemical Cycles*, **15**, 207–225.

Kucharik CJ, Foley JA, Delire C *et al*. (2000) Testing the performance of a dynamic global ecosystem model: water balance, carbon balance and vegetation structure. *Global Biogeochemical Cycles*, **14**, 795–825.

Liski J, Korotkov AV, Prins CFL *et al*. (2003) Increased carbon sink in temperate and boreal forests. *Climatic Change*, **61**, 89–99.

Liski J, Pussinen A, Pingoud K *et al*. (2001) Which rotation length is favourable to carbon sequestration? *Canadian Journal of Forest Research*, **31**, 2004–2013.

Lloyd J, Taylor JA (1994) On the temperature dependence of soil respiration. *Functional Ecology*, **8**, 315–323.

Lucht W, Prentice IC, Myneni RB *et al*. (2002) Climatic control of the high-latitude vegetation greening trend and Pinatubo effect. *Science*, **296**, 1687–1689.

Malanson GP, Cairns DM (1997) Effects of dispersal, population delays, and forest fragmentation on tree migration rates. *Plant Ecology*, **131**, 67–79.

Masera OR, Garza-Caligaris JF, Kanninen M *et al*. (2003) Modelling carbon sequestration in afforestation, agroforestry and forest management projects: the CO2FIX V.2 approach. *Ecological Modelling*, **164**, 177–199.

McGuire AD, Sitch S, Clein JS (2001) Carbon balance of the terrestrial biosphere in the twentieth century: analyses of CO_2, climate and land use effects with four process-based ecosystem models. *Global Biogeochemical Cycles*, **15**, 183–206.

Mearns LO, Giorgi F, McDaniel L *et al*. (2003) Climate scenarios for the Southeastern U.S. based on GCM and regional model simulations. *Climatic Change*, **60**, 7–35.

Morales P, Sykes MT, Prentice IC *et al*. (2005) Comparing and evaluating process-based ecosystem model predictions of carbon and water fluxes in major European forest biomes. *Global Change Biology*, **11**, 2211–2233.

Mücher CA, Steinnocher K, Kressler F *et al*. (2000) Land cover characterization and change detection for environmental monitoring of pan-Europe. *International Journal of Remote Sensing*, **21**, 1159–1181.

Myneni RB, Keeling CD, Tucker CJ *et al*. (1997) Increased plant growth in the northern high latitudes from 1981 to 1991. *Nature*, **386**, 698–702.

Nabuurs GJ, Schelhaas MJ, Mohren GMJ *et al*. (2003) Temporal evolution of the European forest sector carbon sink from 1950 to 1999. *Global Change Biology*, **9**, 152–160.

Nadelhoffer KJ, Emmett BA, Gundersen P (1999) Nitrogen makes a minor contribution to carbon sequestration in temperate forests. *Nature*, **398**, 145–148.

Nakicenovic N, Alcamo J, Davis G *et al*. (2000) *Special Report on Emissions Scenarios: A Special Report of Working Group III of the Intergovernmental Panel on Climate change*. Cambridge University Press, Cambridge.

Nemani RR, Keeling CD, Hashimoto H *et al*. (2003) Climate-driven increases in global terrestrial net primary productivity. *Science*, **300**, 1560–1563.

New M, Hulme M, Jones PD (2000) Representing twentieth century space-time climate variability. Part 2: development of 1901–96 monthly grids of terrestrial surface climate. *Journal of Climate*, **13**, 2217–2238.

NRC (National Research Council – Committee on the Science of Climate Change). (2001) *Climate Change Science: An Analysis of Some Key Questions*. National Academy Press, Washington, DC.

O'Brien K, Sygna L, Haugen JE (2004) Vulnerable or resilient? A multi-scale assessment of climate impacts and vulnerability in Norway. *Climatic Change*, **64**, 193–225.

Parry M (2000) *Assessment of Potential Effects and Adaptation for Climate Change in Europe: The Europe ACACIA project*. Jackson Environment Institute, University of East Anglia, Norwich, UK.

Payne JT, Wood AW, Hamlet AF *et al*. (2004) Mitigating the effects of climate change on the water resources of the Columbia river basin. *Climatic Change*, **62**, 233–256.

Prentice IC, Sykes MT, Cramer W (1993) A simulation model for the transient effects of climate change on forest landscapes. *Ecological Modelling*, **65**, 51–70.

Räisänen J, Hansson U, Ullerstig A *et al*. (2004) European climate in the late twenty-first century: regional simulations with two driving global models and two forcing scenarios. *Climate Dynamics*, **22**, 13–31.

Roeckner E, Bengtsson L, Feitcher J *et al*. (1999) Transient climate change simulations with a coupled atmosphere-ocean GCM including the tropospheric sulfur cycle. *Journal of Climate*, **12**, 3004–3032.

Rounsevell MD, Annetts JE, Audsley E *et al*. (2003) Modelling the spatial distribution of agricultural land use at the regional scale. *Agriculture, Ecosystems and Environment*, **95**, 465–479.

Rowell DP (2006) A demonstration of the uncertainty in projections of UK climate change resulting from regional model formulation. *Climatic Change*, doi: 10.1007/s10584-006-9100-3.

Ruosteenoja K, Tuomenvirta H, Jylhä K (2006) GCM-based regional temperature and precipitation change estimates for Europe under four SRES scenarios applying a super-ensemble pattern-scaling method. *Climatic Change*, in press.

Schaphoff S, Lucht W, Gerten D *et al*. (2006) Terrestrial biosphere carbon storage under alternative climate projections. *Climatic Change*, **74**, 97–122.

Schlesinger WH, Andrews JA (2000) Soil respiration and the global carbon cycle. *Biogeochemistry*, **48**, 7–20.

Schröter D, Cramer W, Leemans R *et al*. (2005) Ecosystem service supply and vulnerability to global change in Europe. *Science*, **310**, 1333–1337.

Sitch S, Smith B, Prentice IC *et al*. (2003) Evaluation of ecosystem dynamics, plant geography and terrestrial carbon cycling in the LPJ Dynamic Global vegetation model. *Global Change Biology*, **9**, 161–185.

Smith B, Prentice IC, Sykes MT (2001) Representation of vegetation dynamics in the modelling of terrestrial ecosystems: comparing two contrasting approaches in European climate space. *Global Ecology and Biogeography*, **10**, 621–638.

Steppeler J, Doms G, Schättler U *et al*. (2003) Meso-gamma scale forecasts using the nonhydrostatic model LM. *Meteorological and Atmospheric Physics*, **82**, 75–96.

Sykes MT, Prentice IC (1996) Climate change, tree species distributions and forest dynamics: a case study in the mixed conifer/northern hardwoods zone of northern Europe. *Climatic Change*, **34**, 161–177.

Tanja S, Berninger F, Vesala T *et al*. (2003) Air temperature triggers the recovery of evergreen boreal forest photosynthesis in spring. *Global Change Biology*, **9**, 1410–1426.

Tsvetsinskaya EA, Mearns LO, Mavromatis T *et al*. (2003) The effect of spatial scale of climatic change scenarios on simulated maize, winter wheat, and rice production in the Southeastern United States. *Climatic Change*, **60**, 37–71.

Waring RH, Running SW (1998) *Forest Ecosystems: Analysis at Multiple Scales*. Academic Press, San Diego, CA.

Zaehle S, Sitch S, Smith B *et al*. (2005) Effects of parameter uncertainties on the modelling of terrestrial biosphere dynamics. *Global Biogeochemical Cycles*, **19**, GB3020.

Zheng D, Freeman M, Bergh J *et al*. (2002) Production of *Picea abies* in south-east Norway in response to climate change: a case study using process-based model simulation with field validation. *Scandavian Journal of Forest Research*, **17**, 35–46.